OFFICE OF NAVAL RESEARCH

Grant N00014-90-J-1193

TECHNICAL REPORT No. 38

Spectral and Temporal Distribution of Phase-Conjugated Fluorescent Photons

by

Henk F. Arnoldus and Thomas F. George

Prepared for publication

in

Journal of Modern Optics

Departments of Chemistry and Physics
State University of New York at Buffalo
Buffalo, New York 14260

December 1990

UNCLASSIFIED
SECURITY CLASSIFICATION OF THIS PAGE

REPORT DOCUMENTATION PAGE

Form Approved
OMB No. 0704-0188

1a. REPORT SECURITY CLASSIFICATION Unclassified	1b. RESTRICTIVE MARKINGS
2a. SECURITY CLASSIFICATION AUTHORITY	3. DISTRIBUTION/AVAILABILITY OF REPORT Approved for public release; distribution unlimited
2b. DECLASSIFICATION/DOWNGRADING SCHEDULE	
4. PERFORMING ORGANIZATION REPORT NUMBER(S) U/BUFFALO/DC/90/TR-38	5. MONITORING ORGANIZATION REPORT NUMBER(S)
6a. NAME OF PERFORMING ORGANIZATION Depts. Chemistry & Physics State University of New York 6b. OFFICE SYMBOL (If applicable)	7a. NAME OF MONITORING ORGANIZATION
6c. ADDRESS (City, State, and ZIP Code) Fronczak Hall, Amherst Campus Buffalo, New York 14260	7b. ADDRESS (City, State, and ZIP Code) Chemistry Program 800 N. Quincy Street Arlington, Virginia 22217
8a. NAME OF FUNDING/SPONSORING ORGANIZATION Office of Naval Research 8b. OFFICE SYMBOL (If applicable)	9. PROCUREMENT INSTRUMENT IDENTIFICATION NUMBER Grant N00014-90-J-1193
8c. ADDRESS (City, State, and ZIP Code) Chemistry Program 800 N. Quincy Street Arlington, Virginia 22217	10. SOURCE OF FUNDING NUMBERS PROGRAM ELEMENT NO. / PROJECT NO. / TASK NO / WORK UNIT ACCESSION NO.

11. TITLE (Include Security Classification)
Spectral and Temporal Distribution of Phase-Conjugated Fluorescent Photons

12. PERSONAL AUTHOR(S)
Henk F. Arnoldus and Thomas F. George

13a. TYPE OF REPORT	13b. TIME COVERED	14. DATE OF REPORT (Year, Month, Day)	15. PAGE COUNT
	FROM _____ TO _____	December 1990	25

16. SUPPLEMENTARY NOTATION
Prepared for publication in the *Journal of Modern Optics*

17. COSATI CODES			18. SUBJECT TERMS (Continue on reverse if necessary and identify by block number)
FIELD	GROUP	SUB-GROUP	PHASE-CONJUGATED FLUORESCENCE; SPECTRAL DISTRIBUTION; PHOTONS; TWO LORENTZIANS; FOUR-WAVE MIXING; TEMPORAL DISTRIBUTION

19. ABSTRACT (Continue on reverse if necessary and identify by block number)

Spontaneous emission of fluorescence radiation by an atom near the surface of a four-wave mixing phase conjugator is considered. It is shown that the spectral photon distribution consists of two Lorentzians, which have their peaks symmetrically located at the two sides of the pump frequency ω of the nonlinear crystal. With ω_0 the atomic resonance, the line at $2\omega-\omega_0$ is more than twice as strong as the line at ω_0. When the phase-conjugate reflectivity exceeds unity, the temporal photon distribution exhibits nonclassical behavior. Then, antibunching of photons prevails, and the photon statistics is sub-poissonian.

20. DISTRIBUTION/AVAILABILITY OF ABSTRACT ☒ UNCLASSIFIED/UNLIMITED ☒ SAME AS RPT ☐ DTIC USERS	21. ABSTRACT SECURITY CLASSIFICATION Unclassified
22a. NAME OF RESPONSIBLE INDIVIDUAL Dr. David L. Nelson	22b. TELEPHONE (Include Area Code) (202) 696-4410 22c. OFFICE SYMBOL

DD Form 1473, JUN 86 *Previous editions are obsolete.*

SECURITY CLASSIFICATION OF THIS PAGE
UNCLASSIFIED

Journal of Modern Optics, in press

SPECTRAL AND TEMPORAL DISTRIBUTION OF PHASE-CONJUGATED FLUORESCENT PHOTONS

Henk F. Arnoldus
Department of Physics
Mendel Hall
Villanova University
Villanova, Pennsylvania 19085, U.S.A.

and

Thomas F. George
Departments of Chemistry and Physics & Astronomy
239 Fronczak Hall
State University of New York at Buffalo
Buffalo, New York 14260, U.S.A.

Abstract. Spontaneous emission of fluorescence radiation by an atom near the surface of a four-wave mixing phase conjugator is considered. It is shown that the spectral photon distribution consists of two Lorentzians, which have their peaks symmetrically located at the two sides of the pump frequency $\bar{\omega}$ of the nonlinear crystal. With ω_o the atomic resonance, the line at $2\bar{\omega}-\omega_o$ is more than twice as strong as the line at ω_o. When the phase-conjugate reflectivity exceeds unity, the temporal photon distribution exhibits nonclassical behavior. Then, antibunching of photons prevails, and the photon statistics is sub-poissonian.

1. Introduction

When two strong counterpropagating laser beams with frequency $\bar{\omega}$ pump a nonlinear crystal, then this device operates as a phase conjugator (PC) for weak incident radiation on its surface, due to a four-wave mixing process in the medium. In particular, the electromagnetic vacuum field interacts with the pump beams, and this results in a spontaneous emission of photons with frequency $\bar{\omega}$ in all directions [1]. When a two-state atom with level separation $\hbar\omega_o$ is located in the vicinity of the surface of the PC, it can absorb these photons. This leads to spontaneous excitation of the atom [2,3] through a three-photon process, as illustrated in Fig. 1. An atom in its ground state $|g\rangle$ absorbs a photon with frequency $\bar{\omega}$, and subsequently emits spontaneously a photon with frequency $2\bar{\omega}-\omega_o$. The energy-conserving diagram is completed by a second absorption of a photon with frequency $\bar{\omega}$, which leaves the atom in the excited state $|e\rangle$. This process is reminiscent of the generation of the three-photon line in resonance fluorescence by an atom in a laser field with frequency $\bar{\omega}$ [4]. After this excitation, the atom decays spontaneously in the usual way, which produces a photon with frequency ω_o. Continuous repetition of this cycle should lead to a steady emission of photons with frequencies ω_o and $2\bar{\omega}-\omega_o$.

The above interpretation of spontaneous emission by an atom near a PC is simply based on energy conservation. We shall show that the fluorescence spectrum consists indeed of two lines, which are positioned at ω_o and $2\bar{\omega}-\omega_o$. Furthermore, we shall evaluate the two-photon correlation function. The antibunching between two ω_o-photons and between two $2\bar{\omega}-\omega_o$-photons then reveals the alternating character of the two emission mechanisms from Fig. 1.

2. Fluorescence

The surface of the PC is taken as the xy-plane, and the atom with dipole moment $\underset{\sim}{\mu}(t)$ is located on the positive z-axis at z = h. The positive-frequency part of the fluorescence radiation field is given by [5]

$$\underset{\sim}{E}(\underset{\sim}{r},t)^{(+)} = \omega_0^2 \frac{e^{-i\omega_o\tau}}{4\pi\varepsilon_o rc^2}\{\underset{\sim}{M}(t) - \underset{\sim}{\hat{r}}(\underset{\sim}{\hat{r}}\cdot M(t))\] \quad , \tag{1}$$

in the far zone. Here,

$$\tau = (h/c)\cos\theta \quad , \tag{2}$$

and the operator $\underset{\sim}{M}(t)$ is defined as

$$\underset{\sim}{M}(t) = \underset{\sim}{\mu}(t)^{(+)} - P^{*}e^{-2i\bar{\omega}t}\underset{\sim}{\mu}(t)^{(-)} \quad , \tag{3}$$

in terms of the positive- and negative-frequency parts of the dipole operator, and the Fresnel reflection coefficient P for a plane wave with frequency ω_o. We have suppressed the retardation with -r/c. Equation (1) was derived by solving the Maxwell-Heisenberg equations for a dipole near the surface of a PC. The term proportional to $\underset{\sim}{\mu}(t)^{(+)}$ is dipole radiation by an atom in empty space. This radiation reflects at the surface, with reflection coefficient P, and this produces the second term. Due to the phase conjugation, $\underset{\sim}{\mu}^{(+)}$ is reflected as $\underset{\sim}{\mu}^{(-)}$, and the factor $\exp(-2i\bar{\omega})$ accounts for the two $\bar{\omega}$ photons in Fig. 1.b.

We shall assume that the radiation passes a polarizer, which transmits the $\underset{\sim}{e}_d$ -component of the field (with $\underset{\sim}{e}_d^{*}\cdot\underset{\sim}{e}_d = 1$). This component is

$$\mathscr{E}(t)^{(+)} = \underset{\sim}{E}(\underset{\sim}{r},t)^{(+)}\cdot\underset{\sim}{e}_d^* = \omega_o^2\frac{e^{-i\omega_o\tau}}{4\pi\epsilon_o rc^2}\underset{\sim}{M}(t)\cdot\underset{\sim}{e}_d^* \quad , \tag{4}$$

where we used $\underset{\sim}{e}_d^* \cdot \hat{\underset{\sim}{r}} = 0$. A photomultiplier then counts photons from this filtered field. With $\underset{\sim}{\mu}_{eg} = \langle e|\underset{\sim}{\mu}|g\rangle$, assumed to be real, the field becomes

$$\mathscr{E}(t)^{(+)} = \omega_o^2\frac{e^{-i\omega_o\tau}}{4\pi\epsilon_o rc^2}(\underset{\sim}{\mu}_{eg}\cdot\underset{\sim}{e}_d)^*\{d^\dagger(t) - P^* e^{-2i\bar{\omega}t}d(t)\} \quad , \tag{5}$$

in terms of the atomic raising operator $d = |e\rangle\langle g|$.

3. Equation of motion

The atomic density operator $\rho(t)$ obeys the Liouville equation

$$i\frac{d\rho}{dt} = (L_a - i\Gamma)\rho \quad , \quad \rho^\dagger = \rho \quad , \quad Tr\rho = 1 \quad , \tag{6}$$

where L_a and Γ represent the free evolution and relaxation, respectively. With the atomic Hamiltonian given by

$$H_a = \hbar\omega_e P_e + \hbar\omega_g P_g \quad , \tag{7}$$

in terms of the projectors $P_e = |e\rangle\langle e|$ and $P_g = |g\rangle\langle g|$ onto the excited state and ground state, respectively, the Liouvillian L_a becomes

$$L_a\sigma = \hbar^{-1}[H_a,\sigma] = \omega_o[P_e,\sigma] \quad . \tag{8}$$

Here we used $P_e + P_g = 1$ and $\omega_o = \omega_e - \omega_g$. Equation (8) defines the action of L_a on an arbitrary Hilbert-space operator σ, rather than on the density operator ρ only. The relaxation operator is [6]

$$\Gamma\sigma = \frac{1}{2}A_e\{P_e\sigma + \sigma P_e - 2d^\dagger\sigma d\} + \frac{1}{2}A_g\{P_g\sigma + \sigma P_g - 2d\sigma d^\dagger\} \quad . \tag{9}$$

in terms of the relaxation constants for the excited state and ground state

$$A_e = A(1 + \frac{1}{2}|P|^2) \quad , \tag{10}$$

$$A_g = \frac{1}{2}A|P|^2 \quad , \tag{11}$$

respectively. The parameter A is the Einstein coefficient for spontaneous decay in empty space.

Of particular interest is the steady-state density operator $\bar{\rho} = \rho(t\to\infty)$, which is the solution of

$$(L_a - i\Gamma)\bar{\rho} = 0 \quad , \quad \bar{\rho}^\dagger = \bar{\rho} \quad , \quad Tr\bar{\rho} = 1 \quad . \tag{12}$$

We readily find

$$\bar{\rho} = \bar{n}_e P_e + \bar{n}_g P_g \quad , \tag{13}$$

in terms of the steady-state level populations

$$\bar{n}_e = \frac{\frac{1}{2}|P|^2}{1 + |P|^2} \quad , \quad \bar{n}_g = 1 - \bar{n}_e \quad . \tag{14}$$

The finite population of the excited state is due to the occurrence of the three-photon process from Fig. 1. The transient solution $\rho(t)$, given an initial state $\rho(0)$, can also be found easily.

4. Fluorescence spectrum

The stationary spectral distribution of photons in a field $\mathcal{E}(t)^{(+)}$ is in general given by

$$J(\omega) = \frac{\zeta}{\pi} Re \int_0^\infty d\tau \; e^{i\omega\tau} < \mathcal{E}(0)^{(-)} \mathcal{E}(\tau)^{(+)} > \quad , \tag{15}$$

where ω is the photon frequency and ζ is an efficiency constant (depending on the aperture of the detector, etc.). The spectrally-unresolved intensity is

$$I = \int d\omega \; J(\omega) = \zeta < \mathcal{E}(0)^{(-)} \mathcal{E}(0)^{(+)} > \quad . \tag{16}$$

which equals the photon counting rate.

With Eq. (5), the field correlation function in Eq. (15) acquires four contributions,

$$\zeta < \mathcal{E}(0)^{(-)} \mathcal{E}(\tau)^{(+)} > = \xi < d(0) d^\dagger(\tau) > + \xi |P|^2 e^{-2i\bar{\omega}\tau} < d^\dagger(0) d(\tau) >$$

$$- \xi P^* e^{-2i\bar{\omega}\tau} < d(0) d(\tau) > - \xi P < d^\dagger(0) d^\dagger(\tau) > \quad . \tag{17}$$

where we introduced the parameter

$$\xi = \zeta \left(\frac{\omega_o^2}{4\pi \epsilon_o r c^2} \right)^2 |\underline{\mu}_{eg} \cdot \underline{e}_d|^2 \quad . \tag{18}$$

The atomic correlation functions in Eq. (17) can be found by transforming first to the

Schrödinger picture. This yields

$$\langle d(0)d^{\dagger}(\tau)\rangle = Trd^{\dagger}e^{-i(L_a - i\Gamma)\tau}(\bar{\rho}d) \quad , \tag{19}$$

and similar expressions hold for the other three correlation functions. With the explicit forms of L_a, Γ and $\bar{\rho}$ from Sec. 3, we obtain

$$\langle d(0)d(\tau)\rangle = \langle d^{\dagger}(0)d^{\dagger}(\tau)\rangle = 0 \quad , \tag{20}$$

$$\langle d(0)d^{\dagger}(\tau)\rangle = \bar{n}_e \, e^{-i\omega_o\tau - \frac{1}{2}(A_e + A_g)\tau} \quad , \tag{21}$$

$$\langle d^{\dagger}(0)d(\tau)\rangle = \bar{n}_g \, e^{i\omega_o\tau - \frac{1}{2}(A_e + A_g)\tau} \quad , \tag{22}$$

for $\tau \geq 0$. Apparently, the last two terms on the right-hand side of Eq. (17) vanish.

Combining everything gives for the fluorescence spectrum

$$\begin{aligned} J(\omega) = {} & \frac{I_e}{\pi} \, Re \, \frac{1}{\frac{1}{2}(A_e + A_g) - i(\omega - \omega_o)} \\ & - \frac{I_g}{\pi} \, Re \, \frac{1}{\frac{1}{2}(A_e + A_g) - i(\omega + \omega_o - 2\bar{\omega})} \quad , \end{aligned} \tag{23}$$

where

$$I_e = \xi \bar{n}_e \quad , \qquad I_g = \xi \bar{n}_g |P|^2 \quad . \tag{24}$$

The spectrum $J(\omega)$ is a sum of two Lorentzians, both with a half-width at half-minimum equal to $\frac{1}{2}(A_e + A_g) = \frac{1}{2}A(1 + |P|^2)$. Similar results were found by Milonni et al [7] and Gaeta and

Boyd [8]. The values of $|P|$ are in the range $0 \leq |P| < \infty$. Therefore, the minimum value of the linewidth is $\frac{1}{2}A$, and this width grows indefinitely with increasing (intensity) reflection $|P|^2$. The first spectral line on the right-hand side of Eq. (23) has a strength equal to I_e, and is located at $\omega = \omega_o$. This line is due to the decay process in diagram (a) from Fig. 1. Notice that I_e is proportional to $\bar{n}_e$, as it should be because the inital state is $|e>$. Similarly, the second line has a strength I_g, and is positioned at $\omega = 2\bar{\omega}-\omega_o$. The responsible process is the three-photon process from diagram (b) in Fig. 1. The line strengths as a function of $|P|^2$ are shown in Fig. 2. Obviously, both I_e and I_g vanish for $|P|^2 \rightarrow 0$. For large reflectivity they behave as

$$I_e/\xi \rightarrow \frac{1}{2} \quad , \qquad I_g/\xi \rightarrow \frac{1}{2}|P|^2 \quad , \tag{25}$$

and it always holds that

$$I_g \geq 2\, I_e \quad , \tag{26}$$

as follows from

$$I_g/I_e = 2 - |P|^2 \quad . \tag{27}$$

When we designate photons in the I_e and I_g lines as "e-photons" and "g-photons", respectively, then Eq. (26) expresses that there are more than twice as much g-photons than there are e-photons. This can be understood as follows. An e-photon is emitted during ordinary spontaneous decay, and it propagates either in the positive or negative z-direction. Since the detector is located in the region $z > 0$, half the number of e-photons can never reach the detector. They travel towards the surface of the PC, and are subsequently annihilated in a four-wave mixing

process inside the medium. The g-photons, on the other hand, always propagate in the positive z-direction. This explains the inequality (26), and the factor of 2. The reason why I_e has an upper limit lies in the fact that the process is ordinary spontaneous decay. When the atom is in $|e\rangle$ at a certain time, it takes a time 1/A to decay and to emit the e-photon. Then the atom has to be excited again during a g-photon emission before it can emit a subsequent e-photon. This limits the emission rate to ½A (for the positive z-direction), and the detection rate to ½ξ. The three-photon process, however, is brought about by stimulated transitions, and its repetition rate can be enhanced unlimitedly by increasing the strength of the "external field" ($\bar{\omega}$-photons).

The spectrally unresolved emission rate is found to be

$$I = I_e + I_g = \frac{1}{2}\xi |P|^2 \frac{3 + |P|^2}{1 + |P|^2} \quad , \tag{28}$$

and its dependence on $|P|^2$ is illustrated in Fig. 3.

6. Photon correlations

The temporal characteristics of the fluorescence photons are most conveniently expressed in terms of the two-photon correlation function $I_2(t_1,t_2)$. By definition, $I_2(t_1,t_2)dt_1dt_2$ equals the probability for the detection of a photon in $[t_1,t_1 + dt_1]$, together with the detection of a photon in $[t_2,t_2 + dt_2]$, but independent of detections at other times. The photon correlation function can be expressed in terms of the incident field on the photomultiplier, according to [9,10]

$$I_2(t_1,t_2) = \zeta^2 \langle \mathscr{E}(t_1)^{(-)} \mathscr{E}(t_2)^{(-)} \mathscr{E}(t_2)^{(+)} \mathscr{E}(t_1)^{(+)} \rangle \quad , \tag{29}$$

for $t_2 \geq t_1$. When the atom is in the steady state $\bar{\rho}$, then $I_2(t_1,t_2)$ depends only on t_1 and t_2 through $t_2 - t_1$, as can be checked by inspection. Therefore, we shall only consider $I_2(0,\tau)$, with $\tau \geq 0$.

With expression (5) for $\mathscr{E}(t)^{(+)}$, we can work out the right-hand side of Eq. (29) and express $I_2(0,\tau)$ in terms of atomic correlation functions. Due to the special form of $\bar{\rho}$, many of these correlation functions turn out to be zero (as in Eq. (20)). It appears that $I_2(0,\tau)$ consists of four terms and can be written as

$$I_2(0,\tau) = \sum_{\alpha\beta} f_{\beta\alpha}(\tau) I_\alpha \quad , \tag{30}$$

where the summation runs over α = e,g and β = e,g. The intensities I_e and I_g are again the intensities of the e-line and the g-line, respectively, and the functions $f_{\beta\alpha}(\tau)$ are defined as

$$f_{\alpha\beta}(\tau) = \frac{1}{I_\alpha} \xi^2 \, Tr R_\beta \, e^{-iL\tau} \, R_\alpha \, \bar{\rho} \quad , \tag{31}$$

with $L = L_a - i\Gamma$. The Liouville operators R_e and R_g are

$$R_e\sigma = d^\dagger \sigma d = P_g \langle e|\sigma|e\rangle \quad , \tag{32}$$

$$R_g\sigma = |P|^2 d\sigma d^\dagger = |P|^2 P_e \langle g|\sigma|g\rangle \quad , \tag{33}$$

for an arbitrary σ. From Eq. (30) and the definition of $I_2(0,\tau)$, it follows that $f_{\beta\alpha}(\tau)I_\alpha$ equals the probability for the detection of a β-photon at time $t = \tau$ and an α-photon at time $t = 0$. Therefore, $f_{\beta\alpha}(\tau)d\tau$ has the significance of the probability for the detection of a β-photon at time τ after the detection of an α-photon at time zero. With the properties

$$\lim_{\tau\to\infty} e^{-iL\tau} \sigma = \bar{\rho} Tr \, \sigma \quad , \tag{34}$$

$$\xi \; Tr \; R_\alpha \; \bar{\rho} \; = \; I_\alpha \quad , \tag{35}$$

which can be verified easily, we find from Eq. (31)

$$\lim_{\tau \to \infty} f_{\beta\alpha}(\tau) \; = \; I_\beta \quad . \tag{36}$$

This relation expresses that for a long delay time τ, the detection of the β-photon becomes independent of the detection of the α-photon. Combination of Eqs. (30) and (36) gives

$$I_2(0,\infty) \; = \; \sum_{\alpha\beta} \; I_\beta I_\alpha \; = \; I^2 \quad , \tag{37}$$

where $I = I_e + I_g$ is the uncorrelated intensity.

The operator R_α can be viewed as the emission operator for an α-photon. Equation (35) expresses that the detection rate I_α for α-photons equals ξ times the expectation value of the operator R_α. The parameter ξ relates the emission rate to the detection rate. This picture is also supported by Eq. (31). Reading from right to left, the atom is initially in state $\bar{\rho}$. The action of R_α then corresponds to the emission of the α-photon. Subsequently, the atomic state evolves over a time τ with exp (-iLτ), after which the action of R_β causes the emission of the β-photon. The factor ξ^2 relates the two emission rates to detection rates. Finally, Eqs. (32) and (33) show explicitly the effect of the action of an emission operator on an atomic density operator. Action of R_e on σ leaves the atom in the ground state, as represented by the projector P_g on $|g\rangle$, and generates the factor $\langle e|\sigma|e\rangle$ which is the population of the excited state. This is precisely what happens in diagram (a) of Fig. 1. The probability for the emission of an e-photon is proportional

to the population of $|e\rangle$, since the atom must be initially in the excited state, and after the emission the atom is in the ground state. Similarly, the action of R_g leaves the atom in $|e\rangle$, and the probability for the emission of a g-photon is proportional to $\langle g|\sigma|g\rangle$, as expressed by Eq. (33). This interpretation is consistent with the processes in diagram (b) of Fig. 1.

Of particular interest is the behavior of $f_{\beta\alpha}(\tau)$ for small values of τ. When $f_{\beta\alpha}(0) > I_\beta$, then the emission of the α-photon enhances the probability for the emission of the subsequent β-photon, as compared to the uncorrelated probability for the emission of a β-photon. When $f_{\beta\alpha}(0) < I_\beta$, then the α-emission reduces the probability for a β-emission. With

$$R_e^2 = R_g^2 = 0 \quad , \tag{38}$$

as follows from Eqs. (32) and (33), we find

$$f_{ee}(0) = f_{gg}(0) = 0 \quad . \tag{39}$$

The relation $f_{ee}(0) = 0$ expresses that the probability for the emission of an e-photon, immediately following an e-emission, is zero. This should be so, because after the emission of the first e-photon the atom is in its ground state, and subsequent emission of an e-photon requires that the atom is in the excited state. This necessary $|g\rangle \rightarrow |e\rangle$ transition is brought about by a three-photon process, which takes a finite time. A similar explanation holds for $f_{gg}(0) = 0$.

For the other two correlation functions, we find

$$\frac{f_{eg}(0)}{I_e} = \frac{1}{\bar{n}_e} > 2 \quad , \tag{40}$$

$$\frac{f_{ge}(0)}{I_g} = \frac{1}{\bar{n}_g} \geq 1 \quad , \tag{41}$$

showing that the emission of an e(g) photon always enhances the probability for the emission of a g(e) photon. Also, this is easily understood. The probability for an e-emission is proportional to the population of $|e\rangle$. For the uncorrelated emission, the atom is in the steady state $\bar{\rho}$, and the population $\bar{n}_e$ is smaller than unity (and, in fact, smaller than 1/2). After a g-emission, however, the atom is in its excited state with certainty. This explains Eq. (40), and a similar interpretation can be given to Eq. (41).

When we do not distinguish between e-photons and g-photons, then we have to consider $I_2(0,\tau)$. For $\tau = 0$ we obtain

$$\frac{I_2(0,0)}{I_2(0,\infty)} = \frac{4}{x}\left(\frac{1+x}{3+x}\right)^2 \quad , \qquad x = |P|^2 \quad , \tag{42}$$

and the corresponding parameter-free curve is shown in Fig. 4. For $0 < |P|^2 < 1$ we have $I_2(0,0) > I_2(0,\infty)$, which means that the emission of the first photon enhances the probability for the emission of a second photon. This behavior is called "bunching", indicating that photons tend to stick together. Antibunching ($I_2(0,0) < I_2(0,\infty)$) occurs for $|P|^2 > 1$. The function $I_2(0,\tau)$ is easily calculated, with the result

$$\frac{I_2(0,\tau)}{I^2} = 1 + g(|P|^2)\, e^{-(A_e+A_g)\tau} \quad , \tag{43}$$

where

$$g(x) = (1-x)\,\frac{x^2 + 3x + 4}{x(x+3)^2} \quad . \tag{44}$$

This correlation function is shown in Fig. 5 for three values of $|P|^2$.

6. Photon statistics

Photon antibunching is a pure quantum feature of radiation, since it cannot be produced by any classical field [11]. A related phenomenon is the possibility that quantum radiation has sub-poissonian photon statistics. This means that the variance $\sigma(t)^2$ in the number of detected photons in [0,t] is smaller than the average $\mu(t)$, which never occurs for classical fields. Mandel introduced the Q-factor [12]

$$Q(t) = \frac{\sigma(t)^2 - \mu(t)}{\mu(t)} \quad , \tag{45}$$

which is negative for sub-poissonian photon statistics. Negative values of Q(t) have been found experimentally in resonance fluorescence [13,14]. For stationary radiation the average is $\mu(t) = It$, with I the intensity. The variance can be expressed in $I_2(0,t)$, and the Q-factor is

$$Q(t) = \frac{2}{It}\int_0^t d\tau\{(t-\tau)I_2(0,\tau) - \tau I^2\} \quad . \tag{46}$$

With Eq. (43) we find for the present problem

$$Q(t) = \frac{2Ig(|P|^2)}{(A_e+A_g)^2 t}\{(A_e+A_g)t - 1 + e^{-(A_e+A_g)t}\} \quad . \tag{47}$$

The sign of Q(t) is given by the sign of $g(|P|^2)$. Therefore, for $|P|^2 > 1$ we have $Q(t) < 1$ for all t, and the statistics is sub-poissonian. For small t we find

$$Q(t) = It\, g(|P|^2) \quad , \qquad t \to 0 \quad , \tag{48}$$

showing that Q(t) increases or decreases linearly with t. For $t \to \infty$, Q(t) reaches the stationary value

$$\bar{Q} = \lim_{t\to\infty} Q(t) = \frac{2Ig(|P|^2)}{A_e + A_g} \quad . \tag{49}$$

Recalling that I, A_e and A_g depend on $|P|^2$, we can then write for the $|P|^2$ dependence of $\bar{Q}$

$$\bar{Q} = \frac{\xi}{A}\frac{1-x}{(1+x)^2} \cdot \frac{x^2 + 3x + 4}{x + 3} \quad , \qquad x = |P|^2 \quad . \tag{50}$$

The factor ξ/A is an efficiency factor. We see that $\bar{Q} = (\xi/A)(4/3)$ for $|P|^2 \to 0$, $\bar{Q} = 0$ for $|P|^2 = 1$, and $\bar{Q} \to -(\xi/A)$ for $|P|^2 \to \infty$. In view of Eq. (45), the value of Q(t) is limited by Q(t)

≥ -1 for any field. The lower limit $Q(t) = -1$ corresponds to $\sigma(t)^2 = 0$, which is the ultimate sub-poissonian limit. By increasing the phase-conjugate reflectivity $|P|^2$, this lower limit can be approached arbitrarily closely, apart from the efficiency factor ξ/A. The dependence of $\overline{Q}A/\xi$ on $|P|^2$ is shown in Fig. 6.

7. Conclusions

We have studied the spectral and temporal properties of fluorescence radiation, which is emitted by an atom near the surface of a PC. The fluorescence spectrum was found to be the sum of two Lorentzians, and the positions of the lines appeared to be consistent with the two relaxation processes shown in Fig. 1. Three-photon processes contribute more than twice as much to the fluorescence yield as compared to ordinary spontaneous decay. From the result for the two-photon correlation function $I_2(0,\tau)$, it followed that the fluorescence photons exhibit antibunching when the reflectivity of the PC exceeds unity. Under the same criterion, the photon statistics is sub-poissonian.

Acknowledgment

This research was supported in part by the Office of Naval Research.

References

[1] Gaeta, A. L., and Boyd, R. W., 1988, Phys. Rev. Lett., 60, 2618.

[2] Cook, R. J., and Milonni, P. W., 1988, IEEE J. Quantum Electron., 24, 1383.

[3] Hendriks, B. H. W., and Nienhuis, G., 1989, Phys. Rev. A, 40, 1892.

[4] Cohen-Tannoudji, C., 1977, Frontiers in Laser Spectroscopy, Proc. 27th Les Houches Summer School, edited by R. Balian, S. Haroche, and S. Liberman (Amsterdam: North-Holland).

[5] Arnoldus, H. F., and George, T. F., 1990, Phys. Rev. A, submitted.

[6] Arnoldus, H. F., and George, T. F., 1990, Phys. Rev. A, submitted.

[7] Milonni, P.W., Bochove, E. J., and Cook, R. J., 1989, J. Opt. Soc. Am. B, 6, 1932.

[8] Gaeta, A.L., and Boyd, R. W., 1990, Coherence and Quantum Optics VI, edited by J. H. Eberly, L. Mandel, and E. Wolf (New York: Plenum), p. 343.

[9] Glauber, R. J., 1965, Quantum Optics and Electronics, edited by C. DeWitt, A. Blandin and C. Cohen-Tannoudji (New York: Gordon & Breach), p. 63.

[10] Kelley, P. L., and Kleiner, W. H., 1964, Phys. Rev., 136, A316.

[11] Paul, H., 1982, Rev. Mod. Phys., 54, 1061.

[12] Mandel, L., 1979, Opt. Lett., 4, 205.

[13] Short, R., and Mandel, L., 1983, Phys. Rev. Lett., 51, 384.

[14] Rempe, G., Schmidt-Kaler, F., and Walther, H., 1990, Phys. Rev. Lett., 64, 2783.

Figure Captions

Fig. 1. Diagram (a) corresponds to ordinary spontaneous decay and the emission of a photon with frequency ω_o. Diagram (b) represents a three-photon process. Two photons with frequency ϖ are absorbed (double lines), and the atom gas goes from the ground state to the excited state. Therefore, the fluorescent photon which is emitted in between the two absorptions must have a frequency $2\varpi-\omega_o$.

Fig. 2. Curves e and g represent the strengths I_e and I_g of the e-line and the g-line, respectively, as a function of the reflectivity $|P|^2$. We have plotted the dimensionless quantities I_e/ξ and I_g/ξ. The dashed lines indicate the asymptotic values ($|P|^2 \rightarrow \infty$).

Fig. 3. Plot of the total intensity I (divided by ξ) as a function of $|P|^2$. The dashed line, at $I/\xi = \frac{1}{2}|P|^2$, is the asymptotic limit.

Fig. 4. Photon correlation function for $\tau = 0$, relative to its value for $\tau = \infty$, as a function of $|P|^2$. For $|P|^2 > 1$ the value of $I_2(0,0)$ is smaller than $I_2(0,\infty)$, which reflects antibunching of photons.

Fig. 5. Curves a, b and c give $I_2(0,\tau)/I^2$ as a function of $(A_e + A_g)\tau$ for $|P|^2 = 0.5$, $|P|^2 = 1$ and $|P|^2 = 4$, respectively. For $|P|^2 = 1$ we have $I_2(0,\tau) = I^2$ for all τ, corresponding to perfectly random (Poisson) detection statistics.

Fig. 6. Plot of the normalized Q-factor, $\overline{QA}/\xi$, as a function of $|P|^2$. For $|P|^2 = 1$ we have $\overline{Q} = 0$, which reflects uncorrelated photon statistics. The dashed line at $\overline{QA}/\xi = -1$ is the asymptotic limit.

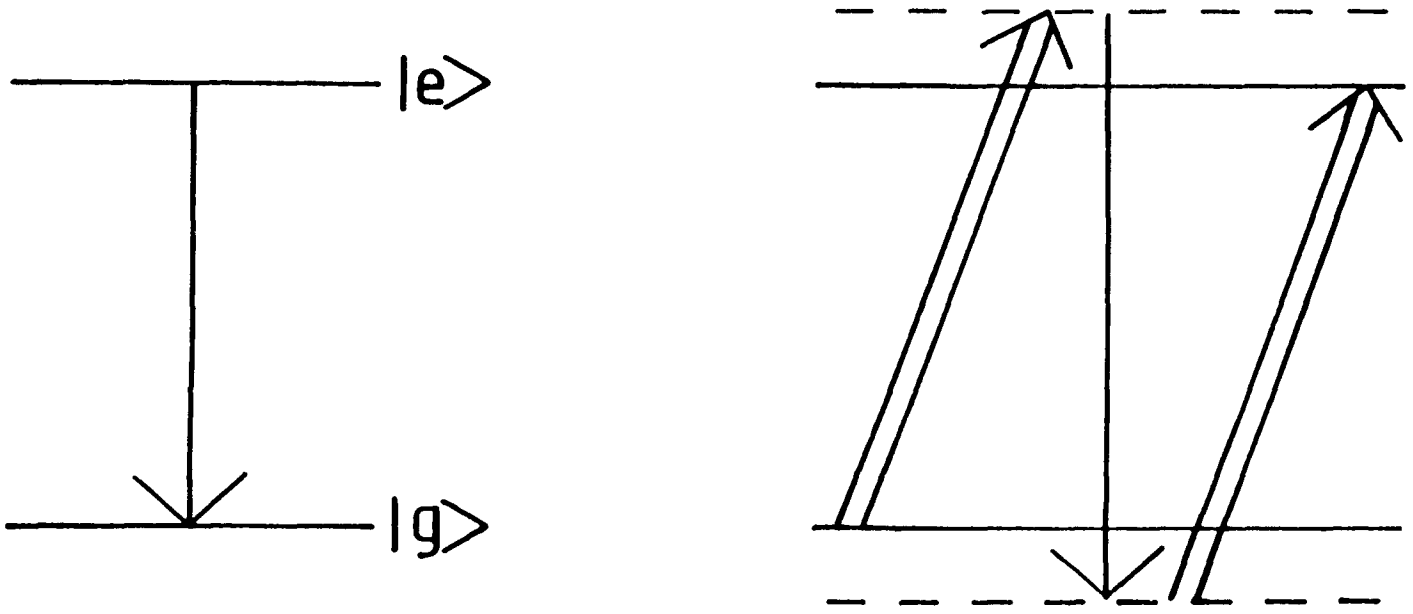

Arnoldus and George, Fig. 1.

Arnoldus and George, fig. 2.

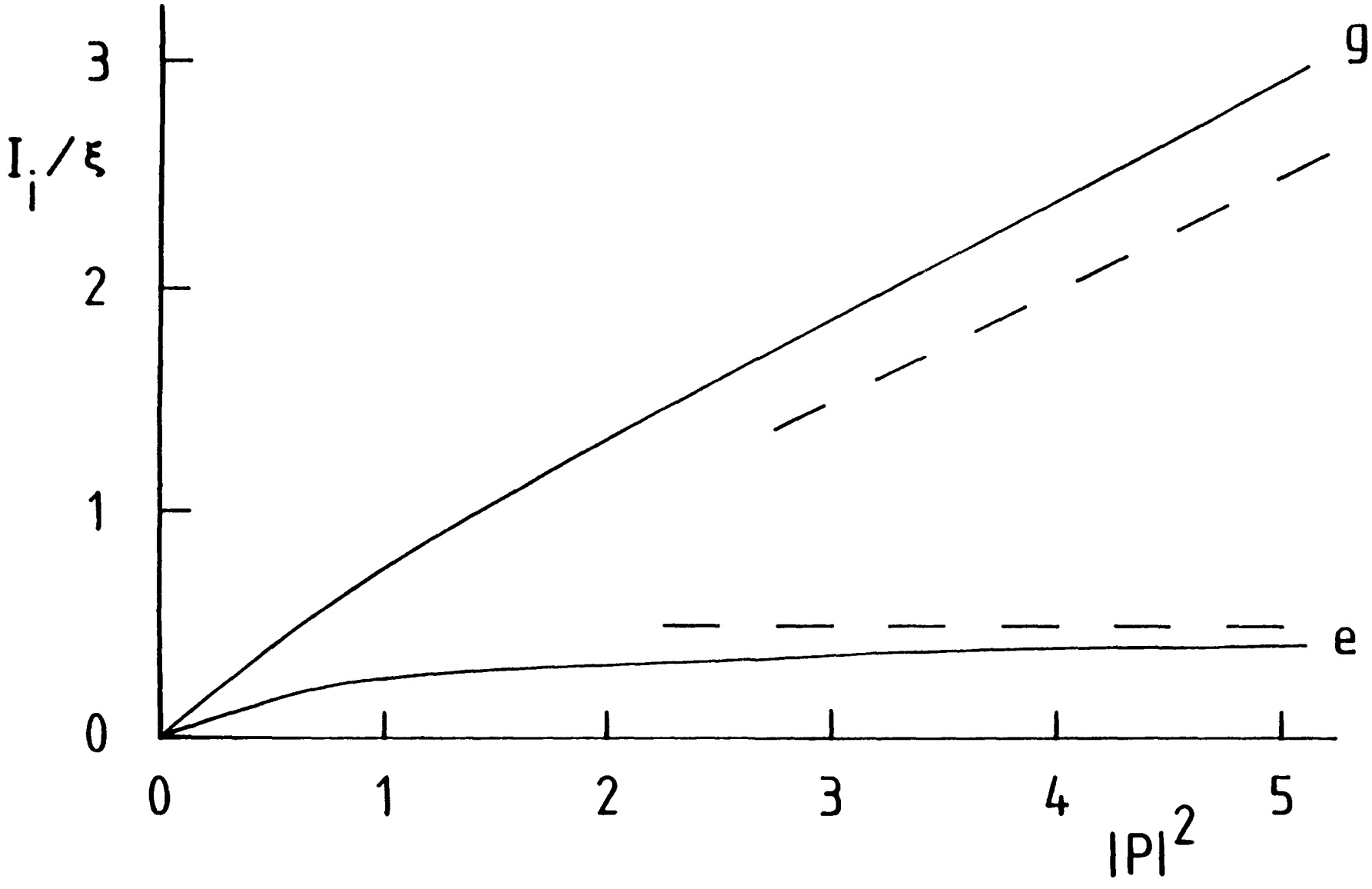

Arnoldus and George, Fig. 3.

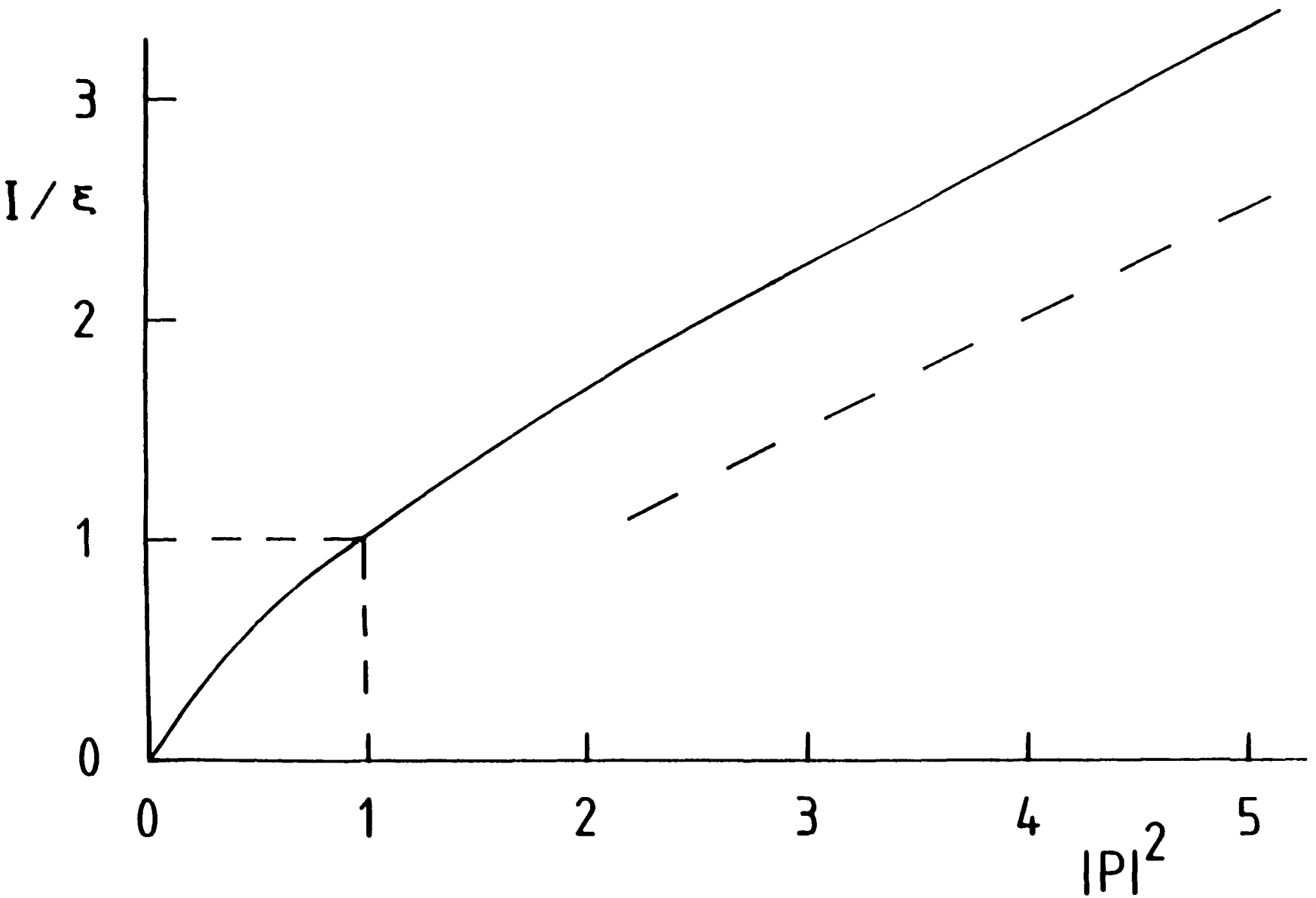

Arnoldus and George, fig. 4.

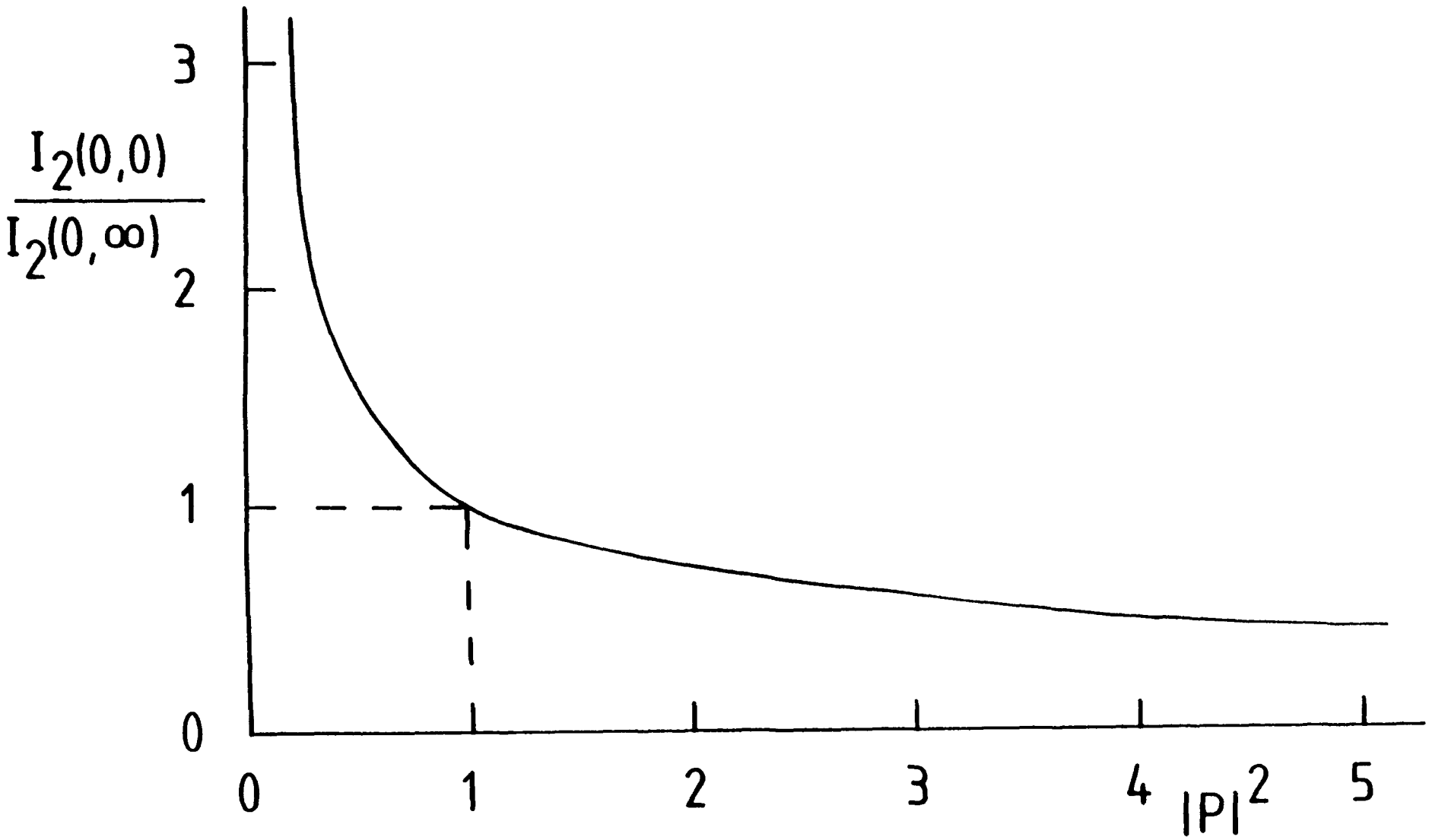

Arnoldus and George, fig. 5.

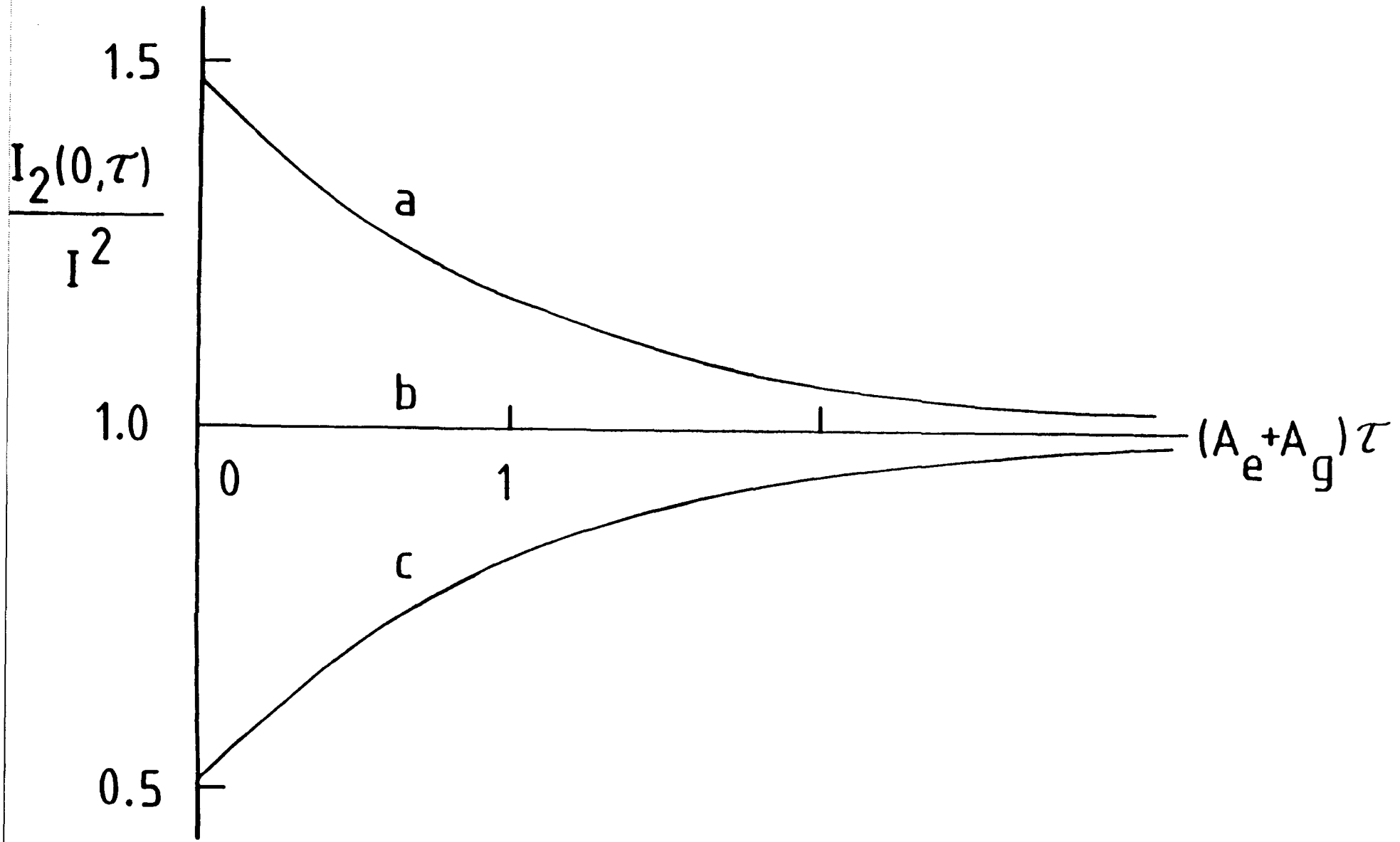

Arnoldus and George, Fig. 6.